JOURNAL OF MATERIALS SCIENCE 20 (1985) 3917–3925

Thermodynamic predictions of the formation of chalcogenide glasses

N. CLAVAGUERA
Fisica del Estado Solido, Facultad de Fisica, Universidad de Barcelona, Diagonal 645, 08028 Barcelona, Spain

M. T. CLAVAGUERA-MORA
Termologia, Facultad de Ciencias, Universidad Autonoma de Barcelona, Bellaterra, Barcelona, Spain

J. ONRUBIA
Termologia, Facultad de Ciencias Fisicas, Universidad de Valencia, Burjassot, Valencia, Spain

The understanding of glass forming ability requires quantitative information on the stable and metastable phase equilibria of binary and multicomponent systems, particularly as a function of composition and temperature. This paper discusses the success of the use of Gibbs free energy curves for the supercooled liquid relative to the stable crystalline phases to describe glass forming ability. Applications are reported for the systems $GeSe_2$–Se, Sb_2Se_3–Se and $GeSe_2$–Sb_2Se_3 for which experimental minimal quenching rates are available. A strongly associated regular solution model for the liquid phase gives a predicted behaviour consistent with experimental data. The method is intended to apply to glass forming liquids both in equilibrium with a solid and in a supercooled state.

1. Introduction

An important part of the applied research on semiconductor glasses has been directed towards ternary or quaternary chalcogenide alloy glasses. However, direct observation of chemical short range order by diffraction methods in these alloys is hindered by the high degree of compositional disorder. As a consequence, the mechanisms responsible for glass-forming ability (GFA) and thermal stability are poorly understood.

A feature shared by all glass-forming melts is a negative heat of mixing, indicative of preferential interaction between unlike constituent atoms. This behaviour suggests that, in the liquid, some of the atoms are free while other atoms associate into small groups or complexes with a composition near to that of the minimum of the heat of mixing [1–10]. A complex may be considered as a molecule A_pB_q. It differs, however, from a real molecule because it is likely to be formed by a group of bonds between atoms rather than by a group of atoms [11]. A rapid quench of the melt freezes the liquid structure and is supposed to fix a definite chemical short range order in the glass.

From the thermodynamic point of view the eutectic crystallization of a melt at a given temperature is driven by the affinity, which measures the Gibbs free energy difference between the liquid and the crystalline phases at that temperature. At the eutectic temperature the minimum value of the affinity occurs at the eutectic composition. This is the basic thermodynamic argument backing the experimental observation that eutectic compositions are in general good glass-formers. However, it is also a general fact that actually the best glass-forming compositions are slightly shifted from the eutectic in many systems.

0022–2461/85 $03.00 + .12

To give some insight to the experimental results on GFA in the $GeSe_2$–Sb_2Se_3–Se system, we derive simplified expressions for the Gibbs free energy of the liquid phase of this system. The molten alloys are assumed to form strongly associated regular (SAR) solutions [10]. The binary interaction parameters between the complexes and their degree of association are deduced by fitting calculated phase diagrams to experimental ones. No ternary interaction parameter is introduced and miscibility in the solid state is neglected. The temperature, T_S, at which the entropy of the liquid phase equals that of the stable crystalline material is calculated as a function of composition by making reasonable estimates of the heat capacity difference between liquid and crystalline phases. Affinities of the binary alloys to undergo eutectic crystallization are calculated in terms of composition at different temperatures. The affinity curves are compared with the experimental minimal quenching rate (MQR) needed to avoid crystallization on cooling the melt from the liquidus temperature.

2. Theoretical résumé

The goal of this study is to discuss and make reasonable predictions on GFA in a simple ternary system like that limited by three simple eutectic type binaries and having a ternary eutectic. Only the main equations are summarized here since details of the underlying theory and model calculations are well established and given elsewhere [10].

The liquid phase is formed by A_pB_q and/or A_rC_s complexes in thermodynamic equilibrium with the (uncombined) A, B and/or C atoms (later we will specifically take A = Se, B = Ge, C = Sb, $p = s = 2$, $q = 1$, $r = 3$). The relationships between the atomic fractions x_i of the elements ($i = 1, 2, 3$) and the mole fractions x_j of the different species (j = A, B, C, A_pB_q, A_rC_s) are

$$\begin{aligned} x_A &= x_1 - [p - x_1(p + q - 1)]x_{A_pB_q} \\ &\quad - [r - x_1(r + s - 1)]x_{A_rC_s} \\ x_B &= x_2 - [q - x_2(p + q - 1)]x_{A_pB_q} \\ &\quad - x_2(r + s - 1)x_{A_rC_s} \\ x_C &= x_3 + x_3(p + q - 1)x_{A_pB_q} \\ &\quad - [s - x_3(r + s - 1)]x_{A_rC_s} \end{aligned} \tag{1}$$

For a SAR-solution it holds that

$$x_A^p x_B^q = x_{A_pB_q} K_1^i \text{ and } x_A^r x_C^s = x_{A_rC_s} K_2^i \tag{2}$$

with the ideal equilibrium constants K_1^i, K_2^i independent of composition.

In the subternary system A–A_pB_q–A_rC_s the solid phase may contain only pure A, A_pB_q and/or A_rC_s crystals. That is, we may assume a negligible solubility range. The mole fractions y_x of the different crystalline phases (X = A, A_pB_q, A_rC_s) are

$$\begin{aligned} y_A &= 1 - y_{A_pB_q} - y_{A_rC_s} \\ y_{A_pB_q} &= \frac{sx_2}{s(qx_1 - px_2 + x_2) + qx_3(1 - r)} \\ y_{A_rC_s} &= \frac{qx_3}{q(sx_1 - rx_3 + x_3) + sx_2(1 - p)} \end{aligned} \tag{3}$$

Vieland's equation for the liquidus boundary of pure compound X can be written as

$$\Delta G^{X \to L} = -RT \ln \Pi_X \tag{4}$$

where $\Delta G^{X \to L}$ is the Gibbs free energy of melting of the compound X at the temperature T and Π_X an activity product given by

$$\begin{aligned} \Pi_A &= a_1 \\ \Pi_{A_pB_q} &= \frac{a_1^p a_2^q}{a_1^{*p} a_2^{*s}} \\ \Pi_{A_rC_s} &= \frac{a_1^r a_3^s}{a_1^{*r} a_3^{*s}} \end{aligned} \tag{5}$$

with a_i ($i = 1, 2, 3$) the activities of the elements in the liquid state relative to pure liquid ($x_i = 1$) at the same temperature and a_i^* the value of a_i at the X stoichiometry.

A ternary system exhibiting a strong tendency for chemical ordering in both the glassy and the liquid state will be treated as a SAR-solution. Consequently, the following approximate expressions for the activity products hold

$$\begin{aligned} \Pi_A &= x_A \exp\{[\alpha_{12} y_{A_pB_q}^2 + \alpha_{13} y_{A_rC_s}^2 \\ &\quad + (\alpha_{12} + \alpha_{13} - \alpha_{23}) y_{A_pB_q} y_{A_rC_s}]/RT\} \\ \Pi_{A_pB_q} &= \frac{x_{A_pB_q}}{x_{A_pB_q}^*} \exp\{[\alpha_{12} y_A^2 + \alpha_{23} y_{A_rC_s}^2 \\ &\quad + (\alpha_{12} + \alpha_{23} - \alpha_{13}) y_A y_{A_rC_s}]/RT\} \\ \Pi_{A_rC_s} &= \frac{x_{A_rC_s}}{x_{A_rC_s}^*} \exp\{[\alpha_{13} y_A^2 + \alpha_{23} y_{A_pB_q}^2 \\ &\quad + (\alpha_{13} + \alpha_{23} - \alpha_{12}) y_{A_pB_q}]/RT\} \end{aligned} \tag{6}$$

where α_{ij} are the interchange energies for the i-j main species with the following correspondence $1 \rightarrow A$, $2 \rightarrow A_pB_q$, $3 \rightarrow A_rC_s$.

The molar Gibbs free energy of the liquid solution is

$$G^L = x_1 G_1^0 + x_2 G_2^0 + x_3 G_3^0 + x_1\, RT \ln a_1 + x_2\, RT \ln a_2 + x_3\, RT \ln a_3 \qquad (7)$$

where G_i^0 is the molar Gibbs free energy of pure liquid i at temperature T. It is related to the Gibbs free energy, G_X^0, of pure compound X by

$$\begin{aligned} G_1^0 - G_A^0 &= \Delta G^{A\rightarrow L} \\ pG_1^0 + qG_2^0 - G^0_{A_pB_q} &= \Delta G^{A_pB_q\rightarrow L} - RT \ln a_1^{*p} a_2^{*q} \\ rG_1^0 + sG_3^0 - G^0_{A_rC_s} &= \Delta G^{A_rC_s\rightarrow L} - RT \ln a_1^{*r} a_3^{*s} \end{aligned} \qquad (8)$$

The gram-atom Gibbs free energy of the solid mixture of crystalline phases is

$$G^S = \frac{y_A G_A^0 + y_{A_pB_q} G^0_{A_pB_q} + y_{A_rC_s} G^0_{A_rC_s}}{y_A + (p+q) y_{A_pB_q} + (r+s) y_{A_rC_s}} \qquad (9)$$

The Gibbs free energy difference between a liquid and a solid mixture of the same average composition, or affinity, $A(T, \mathbf{x}) = G^L - G^S$, can be expressed in terms of the Gibbs free energy of melting and the activity products, using Equations 3 and 8, as

$$A(T, \mathbf{x}) = \frac{\sum_X y_X [\Delta G^{X\rightarrow L} + RT \ln \Pi_X]}{y_A + (p+q) y_{A_pB_q} + (r+s) y_{A_rC_s}} \qquad (10)$$

At the ternary (or binary) eutectic temperature, T_E, there is equilibrium between the liquid (of eutectic composition $\mathbf{x}_E$) and all the crystalline phases. Hence Equation 4 is satisfied for all X, and the affinity, Equation 10, vanishes. Nevertheless, as the liquid composition deviates from $\mathbf{x}_E$, the affinity increases and crystallization of the supercooled liquid will occur if the affinity is large enough. At temperatures lower than T_E stable equilibrium between liquid and crystalline solid is no longer possible and the affinity remains positive in the whole liquid composition range. Nevertheless, $A(T, \mathbf{x})$ still drives the eutectic crystallization of the supercooled liquid (primary crystallization of, let us say, solid A, will be driven by the difference between the chemical potential of A in the liquid solution and in pure solid A).

TABLE I Melting temperatures and enthalpies of fusion of the components

X	T_m (K)	ΔH_m (kcal mol^{-1})	Reference
Se	493	1.4	[13]
$GeSe_2$	1013	4.2	[13, 14]
Sb_2Se_3	888	12.85	[13]

Equation 10 can be used until the glass transition temperature, T_g, is reached. In 1948 Kauzmann [12] guessed that the glass transition had to occur above the temperature T_S at which the entropy of the supercooled liquid, S^L, equals that of the stable crystalline phases, S^S, as it would be absurd to have $S^L < S^S$ (what is called an "entropy catastrophe"). The temperature T_S may be obtained from the following relation

$$\left(\frac{\partial A}{\partial T}\right)_{T=T_S} = 0. \qquad (11)$$

In order to perform that calculation the thermodynamic properties of the supercooled liquid have to be extrapolated at high undercooling.

In the following the relevant features on phase diagram calculations, "ideal" glass transition temperature, T_S, free energy curves and affinity criteria of glass formation will be discussed for the systems $GeSe_2$–Se, Sb_2Se_3–Se and $GeSe_2$–Sb_2Se_3. In all cases the possible type of complexes has been inferred from X-ray diffraction and spectroscopic results in liquid and glassy alloys. The thermodynamic input data used for the calculations are the melting point and the enthalpy of fusion of each crystalline phase, reported in Table I. The Gibbs free energies of the crystalline phases have been taken from Mills [13]. The values of K_1^i, K_2^i and α_{12}, α_{13}, α_{23} have been adjusted to obtain good agreement of the calculated phase diagrams with the experimental ones reported in the literature.

3. Results

3.1. The $GeSe_2$–Se system

We assume the existence of $GeSe_2$ complexes in the liquid phase. This assumption is supported by a wide variety of experimental results on liquid and glassy alloys. Mainly, magnetic

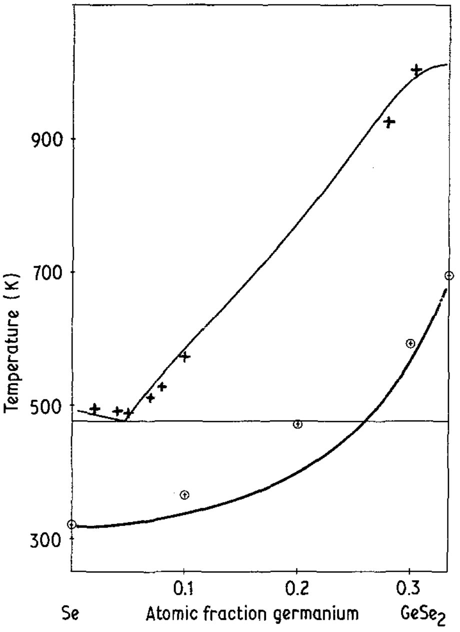

Figure 1 Calculated phase diagram and T_S curves for the GeSe$_2$–Se system. + Experimental phase diagram data after Ipser *et al.* [20]. ⊕ Experimental glass transition temperatures after Bordas *et al.* [21].

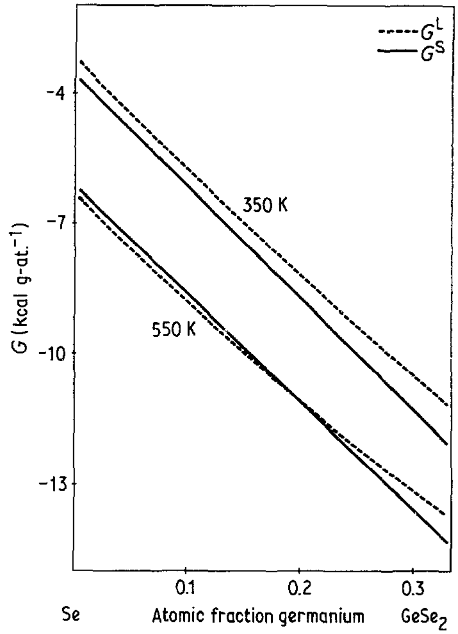

Figure 2 Gibbs free energy curves of supercooled alloy melts, G^L and of crystalline phases, G^S for the system GeSe$_2$–Se.

susceptibility measurements on liquid Se–Ge mixtures show that the introduction of germanium into liquid selenium causes a linkage of chains via four-fold coordinated germanium atoms [15]. Neutron diffraction studies on liquid GeSe$_2$ indicate that the strong covalent bonding between unlike atoms in the solid state still remains on melting [16]. Radial distribution studies on Ge$_x$Se$_{1-x}$ glasses have shown that in the range $0 < x \leqslant 0.4$ the germanium and selenium atoms are respectively four- and two-fold coordinated giving rise to a network structure with GeSe$_{4/2}$ tetrahedral units [17–19].

The calculated phase diagram is shown in the upper part of Fig. 1 together with the experimental points. The best fit is obtained taking for the liquid solution $K_1^l = 10^{-2}$ and $\alpha_{12} = 0.17\,\text{kcal mol}^{-1}$. In order to get a rough estimate of T_S as a function of composition we assume a constant molar heat capacity difference between each liquid and crystalline component (Se and GeSe$_2$) and evaluate ΔC_p by taking $T_S \sim T_g$ for both components. That gives $\Delta C_p^{Se} = 6.5\,\text{cal mol}^{-1}\,\text{K}^{-1}$ and $\Delta C_p^{GeSe_2} = 3.6\,\text{cal g at}^{-1}\,\text{K}^{-1}$. The calculated T_S curve is shown in the lower part of Fig. 1. The points reported there are experimental T_g data. Another estimation of the ΔC_p value can be obtained from the variation of heat capacity in the glass transition region. A change in C_p across the glass transition region of 2.0 to $4.5\,\text{cal g at}^{-1}\,\text{K}^{-1}$ on Ge$_x$Sb$_y$Se$_{1-x-y}$ glasses in the range $0.10 \leqslant x \leqslant 0.35$, $0.05 \leqslant y \leqslant 0.15$ has been reported [22]. These measurements make our assumption quite realistic for GeSe$_2$ but not for Se. The polymeric nature of liquid selenium, neglected here, has certainly to be taken into account to obtain more reliable estimates on ΔC_p.

The Gibbs free energies of the liquid and solid phases, G^L and G^S respectively, are plotted at two different temperatures in Fig. 2. Enthalpy values are referred to those of pure elements (germanium and selenium) at 298.15 K. At 550 K the Gibbs free energy of the liquid equals that of the solid for a composition with ~20 at % Ge. However, the stable state for a sample with that global composition will be a liquid solution with ~10 at % Ge in equilibrium with GeSe$_2$ crystals (as can be found by constructing the common tangent to both the liquid and solid curves). At 350 K the Gibbs free energy of the crystalline phases is lower than that of the liquid solution in the whole composition range. As the difference between G^L and G^S is positive, it exhibits a minimum at a given composition, and there the undercooled liquid can easily become a glass by quenching.

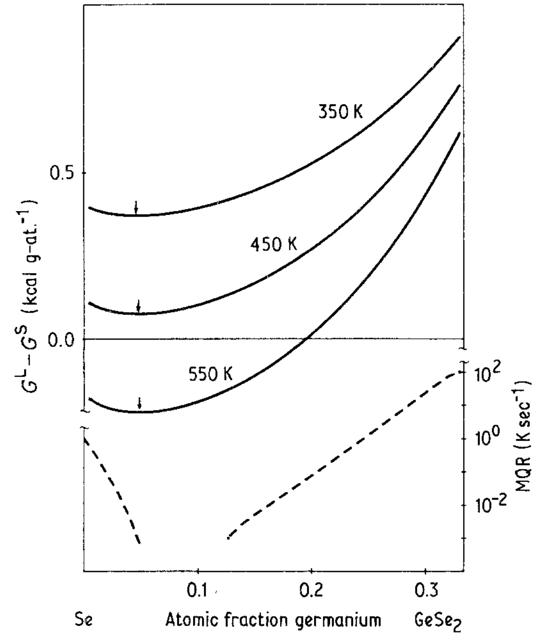

Figure 3 Calculated Gibbs free energy differences $G^L - G^S$ (solid lines) for the system $GeSe_2$–Se. Experimental minimal quenching rate (dashed line) after Bordas *et al.* [21]. Arrows indicate the affinity minima.

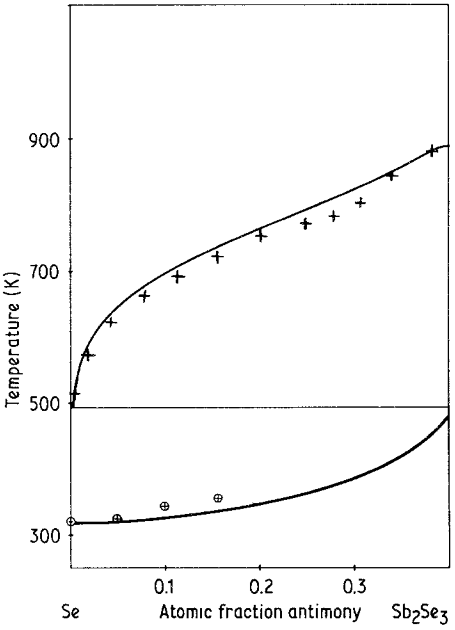

Figure 4 Calculated phase diagram and T_S curves for the Sb_2Se_3–Se system. + Experimental phase diagram data after Meyers and Berkes [24]. ⊕ Experimental glass transition temperatures after Bordas [27].

In fact, $\Delta G = \Delta H - T\Delta S$, so that glass formation is favoured by a great negative value of $H^L - H^S$ and a positive value of $S^L - S^S$. From the value of K_1^i needed to obtain a good agreement between the calculated phase diagram and the experimental one it is evident that chemical ordering is very important in the neighbourhood of pure $GeSe_2$ stoichiometry (33.3 at % Ge). This ordering minimizes the enthalpy of the liquid mixture and will promote liquid $GeSe_2$ as the best glass former in that system. But to the ordering effect one has to add the mixing effect, which maximizes entropy and finally the best glass former composition will be that corresponding to the minimum of the affinity. The affinity as a function of composition at three different temperatures is presented in Fig. 3. At 350 K the affinity minimum corresponds to 4.5 at.% Ge and it shifts to 5.0 at % Ge when the temperature increases to 500 K. To correlate the minimum of the affinity with GFA, experimental data on the MQR needed to obtain glasses in this system are also plotted in the lower part of Fig. 3. There is only a qualitative agreement between the location of the affinity minimum and the compositions that have the lower values of MQR and, as expected, they are not far from the eutectic.

3.2. The Sb_2Se_3–Se system

Evidence of atomic association in the liquid phase, as measured by X-ray diffraction, has been reported [23] for liquid Sb_2Se_3. Furthermore, a highly associated model with Sb_2Se_3 complexes gives an activity for selenium in good agreement with experimental results for liquid mixtures [10]. In order to reproduce both the phase diagram [24] and the activity values [25], the best fit is obtained by taking a SAR-solution model [26]. The experimental phase diagram of this binary system is shown in the upper part of Fig. 4 together with the computed one. The values used for the calculation are those tabulated in Table I and $K_2^i = 10^{-5}$, $\alpha_{13} = 0.9$ kcal mol^{-1}. In the lower part of Fig. 4 are reported both the T_S curve and the experimental glass transition temperatures, T_g. A value of $\Delta C_p^{Sb_2Se_3} = 4.7$ cal g at^{-1} K^{-1} has been introduced in order to calculate T_S.

The Gibbs free energies of liquid and solid phases at 350 and 550 K are plotted in Fig. 5. They have been calculated taking the enthalpy referred to pure elements (antimony and selenium) at 298.15 K. The affinity as a function of composition is presented in the upper part of Fig. 6 at three different temperatures. The Gibbs free energy difference between liquid and

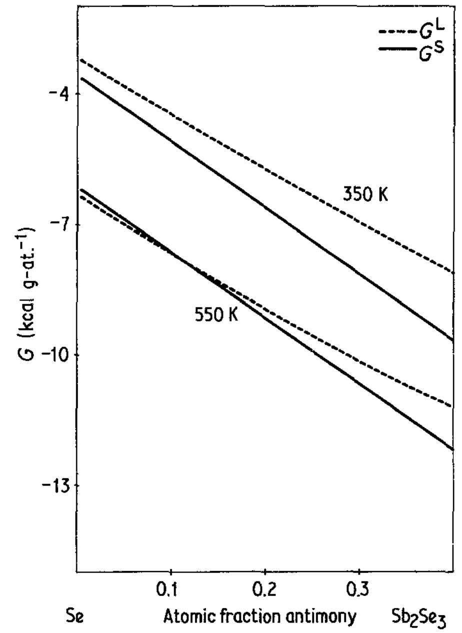

Figure 5 Gibbs free energy curves of supercooled alloy melts, G^L and of crystalline phases, G^S for the system Sb_2Se_3–Se.

crystalline Sb_2Se_3 is significantly higher than that of pure selenium at all three temperatures. The gram-atom entropies of fusion of Se and Sb_2Se_3 being very similar, that comes mainly from the very different values of the melting temperatures of Se and Sb_2Se_3. Then the lower value of the affinity occurs for pure selenium at normal undercooling conditions (between liquidus and glass transition temperatures). There exists a narrow glass-forming region where minimal quenching rates are known [27]. The experimental data are plotted in the lower part of Fig. 6, and confirm that GFA decreases with increasing Sb_2Se_3 content.

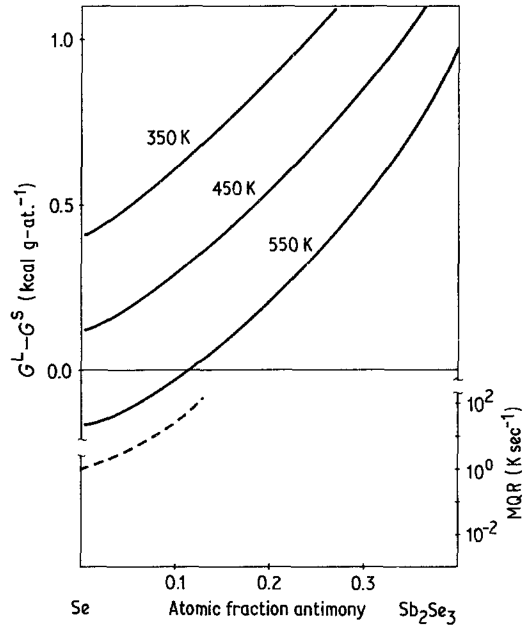

Figure 6 Calculated Gibbs free energy differences $G^L - G^S$ (solid lines) for the system Sb_2Se_3–Se. Experimental minimal quenching rate (dashed line) after Bordas [27].

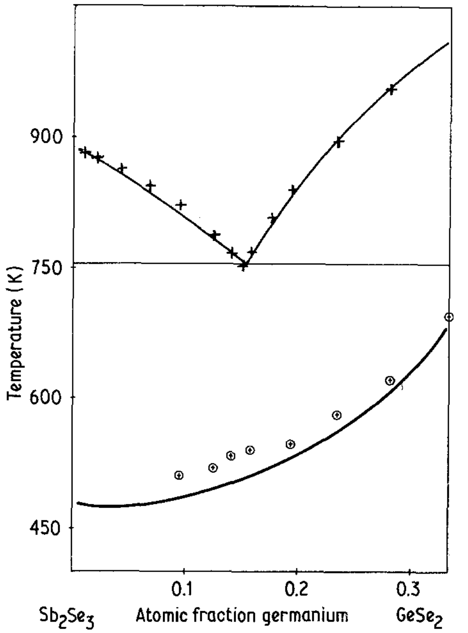

Figure 7 Calculated phase diagram and T_S curves for the $GeSe_2$–Sb_2Se_3 system. + Experimental phase diagram data after Bordas *et al.* [28]. ⊕ Experimental glass transition temperatures after Geli *et al.* [29].

3.3. The Sb_2Se_3–$GeSe_2$ system

The experimental phase diagram of the binary is shown in Fig. 7 together with the computed one. We assume the existence of Sb_2Se_3 and $GeSe_2$ complexes taking, naturally, the same values for the melting temperatures, enthalpies of fusion and K_1^i, K_2^i than in the preceding calculations. We need, however, a new interaction parameter $\alpha_{23} = -1.5\,\mathrm{kcal\,mol^{-1}}$. The "ideal" glass transition temperature, T_S, has been calculated as a function of composition and is plotted in the lower part of Fig. 7 together with the experimental data on glass transition temperature, T_g, for air-quenched glasses of the system.

The Gibbs free energies of the liquid and solid phases are presented, at four different temperatures, in Fig. 8. As expected because of the similarity of the melting temperatures of both components, the Gibbs free energy difference

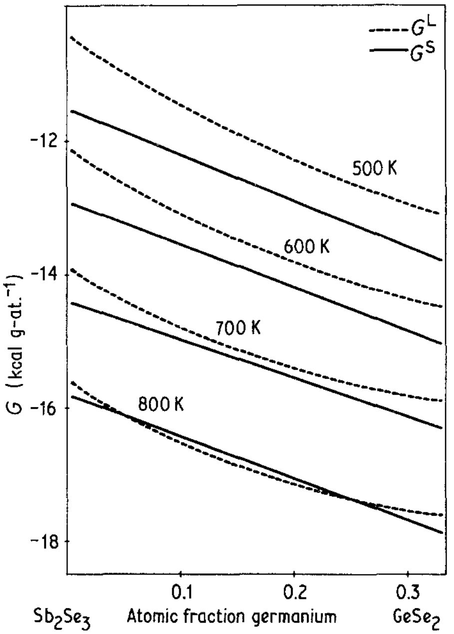

Figure 8 Gibbs free energy curves of supercooled alloy melts, G^L and of crystalline phases, G^S for the system $GeSe_2$–Sb_2Se_3.

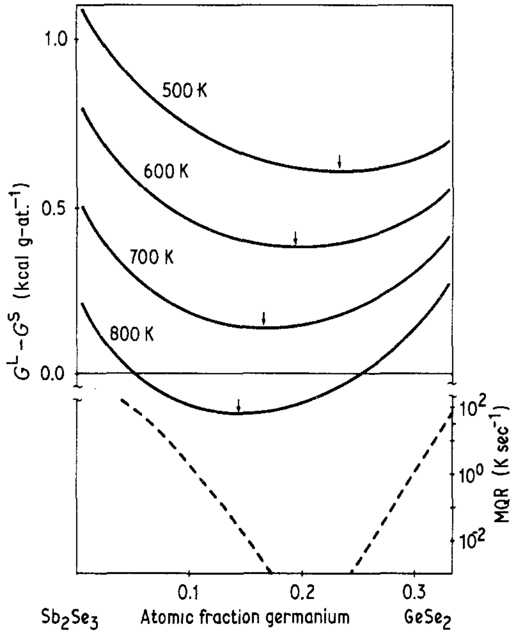

Figure 9 Calculated Gibbs free energy differences $G^L - G^S$ (solid lines) for the system $GeSe_2$–Sb_2Se_3. Experimental minimal quenching rate (dashed line) after Bordas [27].

between liquid and solid phases, at the eutectic temperature, has its minimum value at about half-way between $GeSe_2$ and Sb_2Se_3. However, the gram-atom entropy of fusion of $GeSe_2$ is about one half of that of Sb_2Se_3 and, as a consequence, the affinity minimum will shift towards the GeSe-rich side with increasing undercooling. The affinity values at the four temperatures are shown in Fig. 9. At 800 K the affinity minimum occurs at 14 at % Ge, but as the temperature goes through 700, 600 and 500 K the minimum changes successively to 16, 19 and 23 at % Ge. This result seems to correlate with the experimental MQR data, also plotted in the lower part of Fig. 9, which indicates as best glass-formers in this system those alloys with a composition slightly shifted from the eutectic to higher $GeSe_2$ content. However, it is worth remembering that affinity is a thermodynamic quantity but MQR is really a kinetic parameter.

4. Discussion

To give some insight on GFA we have constructed the affinity curves and correlated them to the MQR needed to avoid crystallization of the molten alloys. Although thermochemical data are rather scarce, it is well known that chemical ordering is very important in liquid and glassy alloys of the systems chosen to do the calculations. The main assumption introduced to obtain the affinity as a function of composition and temperature was to treat the liquid as a SAR-solution. The parameters involved were adjusted to reproduce the experimental phase diagrams. They have a clear physical meaning and the values obtained are consistent with the assumptions made previously. The ideal equilibrium constants K_1^i, K_2^i have values lower than the upper limit needed to undertake strong associated treatment, namely $K_1^i < 10^{-1}$ and $K_2^i < 10^{-2}$ (see [10]). Furthermore the three interchange energies have values $|\alpha_{ij}/RT| \leqslant 0.9$, that is they are small enough for the regular approximation to be valid. It should be noted that, in general, the ideal equilibrium constants depend on the liquid composition, but this is not the case for SAR-solutions [10]. Even if a small temperature dependence can be allowed, due to the fact that increasing temperature diminishes chemical short range order, the ideal equilibrium constants and interchange energies are all assumed constant. With these assumptions we have calculated the affinity as a function of composition for temperatures ranging from about 50 K above the eutectic temperature to about 200 K below it. For completeness, the Gibbs free energies of both liquid and crystalline phase mixture have also been calculated relative to those of pure elements (selenium, germanium and/or antimony).

In as much as there is no definitive definition of GFA we have assumed that it is inversely proportional to the MQR. For this reason the results obtained for the affinity have been compared to experimental MQR data. In the frame of thermodynamics one can argue that below the liquidus temperature the crystallization of a liquid is driven by the affinity, and our attention was focused on possible displacements of the lower values of the affinity from the eutectic composition with increasing undercooling. Other authors have been interested in the calculation of maximum undercooling or glass forming regions, from Gibbs free energy curves, assuming homogenous crystal nucleation theory (see [30] and [31]). For the three binary systems considered here the lower values of the affinity are located near the eutectic composition in normal undercooling conditions. For the Sb_2Se_3–Se system, even at the glass transition temperature the affinity increases monotonically from pure Se to Sb_2Se_3. As mentioned before this behaviour is due mainly to the thermodynamic properties of both components (Se and Sb_2Se_3), because the mixing quantities are too small to have a significant effect. For the $GeSe_2$–Se system the ordering effect is sufficient to balance the importance of the thermodynamic properties of pure components and produces an affinity minimum shifted from pure selenium. This fact is already apparent in the phase diagram, hence as well as in this system as in the Sb_2Se_3–Se system, the lower values of the affinity for each temperature occur at the eutectic composition. In both cases no significant variation with temperature is detected. The most striking feature occurs in the $GeSe_2$–Sb_2Se_3 system. In that system for temperatures 50 K above or below the eutectic temperature the affinity has its minimum value near the eutectic composition. This is at about halfway between $GeSe_2$ and Sb_2Se_3 (16.6 at % Ge) but also at about equal amounts of $GeSe_2$ and Sb_2Se_3 complexes (12.5 at % Ge). Furthermore, the affinity minimum is displaced significantly with temperature. Apart from the properties of pure components, this is a consequence of the decreasing of the mixing entropy contribution ($T\Delta S$) with decreasing temperature.

5. Conclusions

A simplified expression for the affinity of a liquid to crystallize completely has been derived in a ternary system by neglecting miscibility in the solid state and assuming that the liquid phase can be treated as a strongly associated regular solution with particularly simple expressions for the Gibbs free energy reflecting the liquid chemical ordering. This expression has been applied to glass-forming liquids both in equilibrium with a solid and in a supercooled state in order to discuss glass forming ability.

Phase diagram calculations have been done and affinity curves as a function of composition constructed for the systems $GeSe_2$–Se, Sb_2Se_3–Se and Sb_2Se_3–$GeSe_2$. The temperature, T_S, at which the entropy of the supercooled liquid would equal that of the stable crystalline phase has been derived by assuming a temperature-independent heat capacity difference between liquid and solid compounds.

The existence of $GeSe_2$ and/or Sb_2Se_3 complexes in the liquid mixtures was inferred from X-ray diffraction and spectroscopic results reported in the literature. In all cases the calculated phase diagram agrees with the experimental one and the parameters needed for the calculation indicate the correctness of the strongly associated treatment undertaken.

Glass-forming ability was assumed to be inversely proportional to the minimal quenching rate needed to avoid crystallization. For all temperatures between liquidus and glass transition temperature we observe a correlation between the minimum affinity values and the lower values of the minimal quenching rate, both occurring at compositions near the eutectic. Thermodynamic arguments to explain this fact have been put forward.

Acknowledgement

The authors wish to thank Professor R. W. Cahn for encouraging and fruitful discussions and critical reading of the manuscript.

References

1. A. S. JORDAN, *Met. Trans.* **1** (1970) 239.
2. A. LAUGIER, *Rev. Phys. Appl.* **8** (1973) 259.
3. A. BHATIA and W. H. HARGROVE, *Phys. Rev.* **B10** (1974) 3186.
4. A. S. JORDAN, *Met. Trans.* **7B** (1976) 191.
5. A. LAUGIER, G. CHAUSSEMY and J. FORNAZERO, *J. Non-Cryst. Solids* **23** (1977) 419.

6. J. CHOLINSKI, M. LASOCKA and H. MATYJA, *Rev. Phys. Appl.* **12** (1977) 1.
7. F. SOMMER, *Z. Metallkde* **73** (1982) 72, 77.
8. J. D. KELLY, B. G. MARTIN, F. R. SZOFRAN and S. L. SEHOCZKY, *J. Electrochem. Soc.* **129** (1982) 2360.
9. C. BERGMAN, R. CASTANET, H. SAID, M. GILBERT and J. C. MATHIEU, *J. Less-Common Metals* **85** (1982) 121.
10. M. T. CLAVAGUERA-MORA and N. CLAVAGUERA, *J. Phys. Chem. Solids* **43** (1982) 963.
11. M. T. CLAVAGUERA-MORA, N. CLAVAGUERA and J. ONRUBIA, *Calphad* **8** (1984) 163.
12. W. KAUZMANN, *Chem. Phys.* **43** (1948) 219.
13. K. C. MILLS, "Thermodynamic data for Inorganic Sulphides, Selenides and Tellurides" (Butterworths, London, 1974).
14. B. LEGENDRE, Private communication (1982).
15. M. MISONU and H. ENDO, *Ber. Bunsenges-Phys. Chem.* **86** (1982) 645.
16. O. UEMURA, Y. SAGARA, D. MUNO and T. SATOW, *J. Non-Cryst. Solids* **30** (1978) 155.
17. O. UEMURA, Y. SAGARA and T. SATWO, *Phys. Status Solidi* **a26** (1974) 99.
18. R. W. FAWCETT, C. N. J. WAGNER and G. S. CARGILL III, *J. Non-Cryst. Solids* **8/10** (1972) 369.
19. J. C. MALAURENT and J. DIXMIER, *ibid.* **35/36** (1980) 1227.
20. H. IPSER, M. GAMBINO and W. SCHUSTER, *Monatshefte für Chemie* **113** (1982) 389.
21. S. BORDAS, N. CLAVAGUERA, M. D. BARO, M. T. CLAVAGUERA-MORA and J. CASAS-VAZQUEZ, "Thermal Analysis", Proceedings of 5th ICTA, Kyoto, August 1977, edited by H. Chihara (Heyden, London, 1977) p. 18.
22. P. S. L. NARASIMHAM, A. GIRIDAR and S. MAHADEVAN, *J. Non-Cryst. Solids* **43** (1981) 301.
23. T. SATWO, O. UEMURA, S. AKAIKE and S. TAMAKI, *ibid.* **29** (1978) 215.
24. M. B. MEYERS and J. S. BERKES, *ibid.* **8/10** (1972) 804.
25. B. PREDEL, F. GERDES and U. GERLING, *Z. Metallkde* **70** (1979) 109.
26. J. ONRUBIA, PhD thesis, Universidad de Valencia (1983).
27. S. BORDAS, PhD thesis, Universidad Politecnica de Barcelona (1977).
28. S. BORDAS, B. LEGENDRE and M. T. CLAVAGUERA-MORA, *Thermochimica Acta* **56** (1982) 161.
29. M. GELI, S. BORDAS, N. CLAVAGUERA and M. T. CLAVAGUERA-MORA, "Jornadas Cientificas sobre Ceramica y Vidrio", edited by C. de la Fuente (Sociedad Española de Ceramica y Vidrio, Madrid, 1980) p. 196.
30. C. V. THOMSON and F. SPAEPEN, *Acta Metall.* **31** (1983) 2021.
31. N. SAUNDERS and A. P. MIODOWNIK, *Ber. Bunsenges-Phys. Chem.* **87** (1983) 830.

Received 24 September
and accepted 20 November 1984